

Evidence for the Pleistocene Arc Hypothesis from genome-wide SNPs in a Neotropical dry forest specialist, the Rufous-fronted Thornbird (Furnariidae: *Phacellodomus rufifrons*)

Eamon C. Corbett^{1,2}  | Gustavo A. Bravo¹  | Fabio Schunck³  | Luciano N. Naka^{1,4}  | Luís F. Silveira³  | Scott V. Edwards¹ 

¹Department of Organismic and Evolutionary Biology & Museum of Comparative Zoology, Harvard University, Cambridge, MA, USA

²Department of Biological Sciences & Museum of Natural Science, Louisiana State University, Baton Rouge, LA, USA

³Seção de Aves, Museu de Zoologia da Universidade de São Paulo, São Paulo, Brazil

⁴Departamento de Zoologia, Universidade Federal de Pernambuco, Recife, Brazil

Correspondence

Scott V. Edwards, Department of Organismic and Evolutionary Biology & Museum of Comparative Zoology, Harvard University, Cambridge, MA, USA.
Email: sedwards@fas.harvard.edu

Funding information

National Science Foundation –NSF– Division of Environmental Biology, Grant/Award Number: DEB-1831560; Fundação de Amparo à Ciência e Tecnologia do Estado de Pernambuco, Grant/Award Number: APQ-0337-2.04/15; Conselho Nacional de Desenvolvimento Científico e Tecnológico, Grant/Award Number: 302291/2015-6, 308337/2019-0, 432630/2016-3 and 457974-2014-1; São Paulo Research Foundation – FAPESP, Grant/Award Number: 2012-23852-0, 2018/20249-7 and 2017/23548-2; Museum of Comparative Zoology; Harvard College Research Program; Harvard University Center for the Environment

Abstract

South American dry forests have a complex and poorly understood biogeographic history. Based on the fragmented distribution of many Neotropical dry forest species, it has been suggested that this biome was more widely distributed and contiguous under drier climate conditions in the Pleistocene. To test this scenario, known as the Pleistocene Arc Hypothesis, we studied the phylogeography of the Rufous-fronted Thornbird (*Phacellodomus rufifrons*), a widespread dry forest bird with a disjunct distribution closely matching that of the biome itself. We sequenced mtDNA and used ddRADseq to sample 7,167 genome-wide single-nucleotide polymorphisms from 74 *P. rufifrons* individuals across its range. We found low genetic differentiation over two prominent geographic breaks – particularly across a 1,000 km gap between populations in Bolivia and Northern Peru. Using demographic analyses of the joint site frequency spectrum, we found evidence of recent divergence without subsequent gene flow across those breaks. By contrast, parapatric morphologically distinct populations in northeastern Brazil show high genetic divergence with evidence of recent gene flow. These results, in combination with our paleoclimate species distribution modelling, support the idea that currently disjunct patches of dry forest were more connected in the recent past, probably during the Middle and Late Pleistocene. This notion fits the major predictions of the Pleistocene Arc Hypothesis and illustrates the importance of comprehensive genomic and geographic sampling for examining biogeographic and evolutionary questions in complex ecosystems like Neotropical dry forests.

KEY WORDS

ddRADseq, demographic modelling, Furnariidae, phylogeography, seasonally dry tropical forest

1 | INTRODUCTION

Pleistocene climate fluctuations have long been implicated in the generation and structuring of South American biodiversity. The most prominent model regarding these fluctuations is the “Rainforest

Refugia Hypothesis,” which proposes that the fragmentation of the Amazon during cold and dry periods promoted allopatric speciation by separating rainforest birds into disjunct rainforest “refugia” surrounded by open habitats (Haffer, 1969). A complementary proposal, known as the “Pleistocene Arc Hypothesis” (Prado & Gibbs, 1993),

aims to explain the disjunct distributions of widespread species and clades currently found in distinct patches of Seasonally Dry Tropical Forests (SDTF) across the continent. The SDTF biome (hereafter the “dry forest”) is characterized by low annual rainfall and high seasonality, and is found in a number of disjunct regions of the Neotropics (Pennington et al., 2000, 2006). The reasoning behind the arc hypothesis is that although cold dry periods in the Pleistocene may have resulted in the fragmentation of lowland rainforests, those same dry periods would likely have promoted the expansion of dry forests, forming a continuous arc encircling the southern half of Amazonia from Peru to Brazil (Ab’Saber, 1977; Prado & Gibbs, 1993). In warmer and wetter interglacial climates, these dry forests would be restricted to disjunct patches, as they are today.

Data from sediment and ice cores show that the Pliocene (5.33–2.58 Ma) was a relatively warm period, with average temperatures above the present day, whereas the earlier Pleistocene (~2.58–0.77 Ma) was a period of decreasing global temperatures with a 41,000-year glacial cycle (Burke et al., 2018; Clark et al., 2006; Lisiecki & Raymo, 2005). After the mid-Pleistocene transition (1.25–0.7 Ma), the Middle and Late Pleistocene (770–11.7 ka) were characterized by lower average temperatures and more pronounced glacial periods on a 100,000-year cycle, including the Last Glacial Maximum (LGM) ~21,000 years ago (Clark et al., 2006; Hughes et al., 2013; Lisiecki & Raymo, 2005; Petit et al., 1999; Shackleton & Opdyke, 1976). Thus, previously disjunct dry forest patches are most likely to have been connected during the coldest and driest periods of the Middle and Late Pleistocene, although local precipitation dynamics may contribute additional complexity (Baker et al., 2020). These “Pleistocene Arc” periods could have facilitated the expansion of widespread dry forest species across the continent, populations of which would then have been cyclically connected and isolated in synchrony with climate cycles.

The extent to which repeated climate-induced isolation during the Middle and Late Pleistocene may have promoted speciation in rainforest and dry forest species (during glacial and interglacial periods, respectively) is controversial. Some recent molecular data sets have questioned the role of Pleistocene climate fluctuations as drivers of speciation in the Neotropics (Hoorn et al., 2010; Pennington et al., 2004; Rull, 2011; Willis & Whittaker, 2000), in part because these climate cycles are relatively recent compared to the origins of the Neotropical biota (Klicka & Zink, 1997). For instance, divergences of most South American bird sister species pairs have been dated to the earlier Pleistocene or the Pliocene (Naka & Brumfield, 2018; Smith et al., 2014; Weir & Schlüter, 2007). Similarly, studies using primarily mitochondrial and plastid genes have found pre-Pleistocene divergences between disjunct populations of plant and lizard species in dry forests (Cortes et al., 2015; Lanna et al., 2018; Pennington et al., 2004; Werneck et al., 2009).

These results suggest that Pleistocene climatic cycles are likely to have generated intraspecific structure between disjunct dry forest populations rather than interspecific divergence (Avise & Walker, 1998; Mogni et al., 2015). Unfortunately, few phylogeographic studies of widespread dry forest species are available, and

those that have been published have produced conflicting results. Although studies in dry forest lizards (Werneck et al., 2012) and plants (Caetano et al., 2008; Collevatti et al., 2012) indicated divergences between populations predating the Pleistocene, studies of birds (Savit & Bates, 2015) and flies (Moraes et al., 2009) have suggested Middle to Late Pleistocene divergences between populations. Support for the arc hypothesis has also come from genetic studies on two dry forest specialist woody plants, *Tabebuia impetiginosa* and *Astronium urundeuva*, the population sizes of which are inferred to have increased at the Last Glacial Maximum (Caetano et al., 2008; Collevatti et al., 2012). However, a similar study on the widespread dry forest tree *Tabebuia rosealba* found evidence for a population contraction at the LGM, contradicting a main prediction of the arc hypothesis (de Melo et al., 2016).

Evidence from palynological analyses, paleontology, and distribution modelling of multiple species further complicates the picture. Palynological evidence suggests that some dry forests, such as the Chiquitania of Bolivia, may have formed relatively recently, thus contrasting with the idea that the current period is one of minimum historical extent for the biome in the Neotropics (Behling, 1998; Mayle, 2004). On the other hand, paleontological analysis of Late Pleistocene bird fossils has suggested the past expansion of dry forests in some areas, including the dry Tumbesian forests of Peru (Oswald & Steadman, 2015). Although paleoclimate species distribution models of some dry forest species indicate greater range connectivity during the LGM and other Quaternary dry periods (Collevatti et al., 2012; Savit & Bates, 2015), other analyses have suggested range contraction during the same period (Arruda et al., 2018; Mayle, 2004; de Melo et al., 2016). Still other studies predicted a more complex pattern, with less historical connectivity through the Brazilian Cerrado but a greater extent of dry forest along the southwest fringes of the Amazon abutting the Andes (Werneck et al., 2011, 2012).

The ability to sequence thousands of genetic markers now allows for the level of fine-scale resolution of intraspecific population structure that is necessary to examine the influence of events as recent as Middle and Late Pleistocene climate fluctuations (Carstens et al., 2013; Edwards et al., 2015; Hickerson et al., 2010; McCormack et al., 2013; Richards et al., 2007). Although these techniques have begun to be used to tackle questions of Neotropical dry forest biogeography and population differentiation (Oswald et al., 2017; Termignoni-García et al., 2017), they have not been previously applied to dry forest species that are widespread across South America. Doing so will provide a greater understanding of the genetic structuring of dry forest species with large, noncontiguous distributions, and of the history of the dry forest biome itself.

If we are to find the signatures of a recent “Pleistocene Arc” event, then it is likely to be between closely related but geographically disjunct populations of widespread species. One such species is the Rufous-fronted Thornbird (Furnariidae: *Phacellodomus rufifrons*), a common and widespread dry forest and open habitat bird. Although this relatively small and drab furnariid is often overlooked in its habitat, its remarkably large stick nests are a

conspicuous and characteristic feature of many Neotropical dry forests (Remsen, 2003a; Ridgely & Tudor, 2009; Skutch, 1969). *Phacellodomus rufifrons* has six described subspecies (Dickinson & Christidis, 2014; Remsen, 2003a), mirroring the distribution of dry forests around Amazonia (See Figure 1 and Supporting information). The northernmost two subspecies, *castilloi* and *inornatus* from the Llanos of Colombia and Venezuela, lack the eponymous rufous forehead and are considered by some sources to represent a distinct species (Boesman, 2016; del Hoyo, Collar, & Kirwan, 2017; Hilty, 2003; Ridgely & Tudor, 2009). The distribution of the "southern" subspecies of *P. rufifrons* (used hereafter to refer to *peruvianus*, *sincipitalis*, *rufifrons*, and *specularis*) is a close match with that of the tree species *Anadenathera colubrina*, the quintessential dry forest plant species most often used to illustrate the arc pattern (Mogni et al., 2015; Prado & Gibbs, 1993). This makes *P. rufifrons* well-suited to be used as a model species for investigating the arc hypothesis.

The dispersal ability of a species – both in terms of its ability to travel long distances and its ability to cross unsuitable habitat – will affect how it responds to geological events, including

climate-driven changes in habitat distribution (Smith et al., 2014). Among birds *P. rufifrons* is predicted to have a low dispersal capability, as it is a nonmigratory species with rounded wings and forages largely on the ground (Claramunt et al., 2012; Remsen, 2003a; Skutch, 1969). Although *P. rufifrons* can tolerate relatively high levels of human habitat disturbance and inhabits a variety of dry environments, it does not occur in tropical rainforest (Remsen, 2003a). Based on these traits, *P. rufifrons* is expected to be relatively unlikely to disperse between disjunct regions of dry forest. Its evolutionary history is thus expected to be more closely linked to the historical distribution of the biome than would be expected in more vagile bird species.

There are three primary scenarios that could explain the present-day distribution of *P. rufifrons*, each of which makes certain predictions about the genetic structure and demographic history of the species. The first is that the currently disjunct populations of *P. rufifrons* have been isolated for a relatively long time, predating Pleistocene climate cycles. This scenario would produce deep mitochondrial divergences between populations, clear genomic

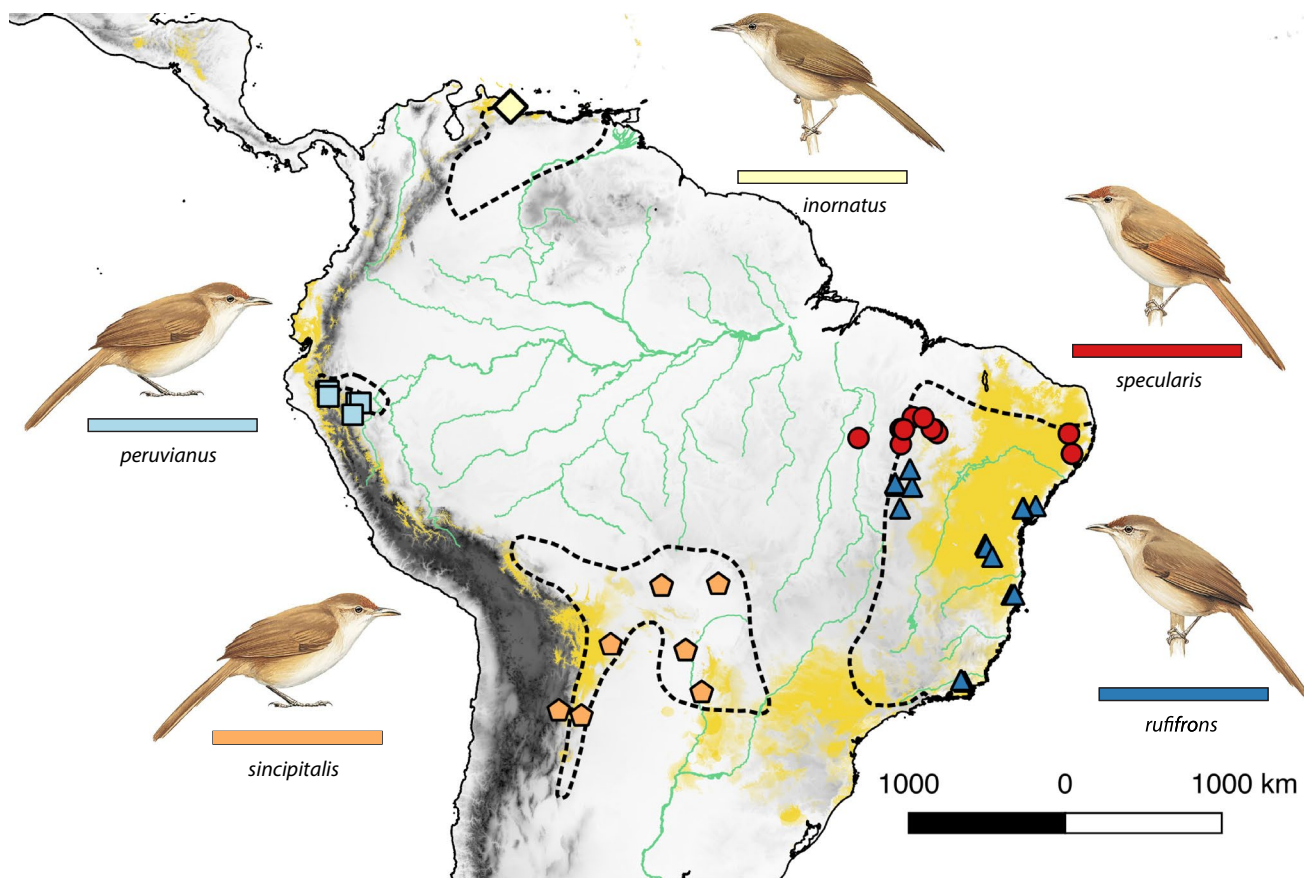


FIGURE 1 Range and sampling localities of *Phacellodomus rufifrons*, showing a highly disjunct distribution that corresponds to the extent of the dry forest biome. Shaded regions in yellow represent the modelled current distribution of seasonally dry tropical forests, adapted from Särkinen et al. (2011). Dotted outlines represent the estimated current distribution of *P. rufifrons* (adapted from Birdlife International). Red circles represent samples of the subspecies *specularis*; dark blue triangles *rufifrons*; orange pentagons *sincipitalis*; light blue squares *peruvianus*, and the yellow diamond *inornatus*. Subspecies *castilloi* from the Llanos was not sampled. Bird illustrations were provided with permission by the team of the Handbook of Birds of the World at Lynx Edicions [Colour figure can be viewed at wileyonlinelibrary.com]

structure, and little evidence for modern gene flow between populations, which would be essentially on divergent evolutionary trajectories.

The second scenario would be concordant with the Pleistocene Arc Hypothesis, that the present-day disjunct populations of *P. rufifrons* were intermittently connected during dry periods in the Middle and Late Pleistocene. Under this scenario we would expect shallow mitochondrial divergences between populations and weak genomic structuring. However, we would not expect present-day gene flow between populations. Crucially, we would expect the relative relatedness between populations to be correlated not to the present-day degree of disjunction between them, but to the past suitability of the intervening habitat for *P. rufifrons*. We also might expect to find evidence for fluctuations in population sizes through the Pleistocene.

A third scenario would be that the currently disjunct populations of *P. rufifrons* have never been connected, and long-distance dispersal to distant patches of suitable habitat is responsible for its current distribution. This can be difficult to distinguish with certainty from the previous alternatives, but there are some patterns that would be more likely under a dispersal-only scenario. For example, we might expect to find signatures of population bottlenecks or founder effects if long-distance dispersal of a small number of individuals gave rise to entire populations. Additionally, if *P. rufifrons* is capable of dispersing across the large gaps in its current range, then we would expect some degree of ongoing dispersal, and present-day gene flow proportional to the distance between populations.

Here, we used model-based analyses of genome-wide data from disjunct *P. rufifrons* populations across the species' range to test the expectations of the Pleistocene Arc Hypothesis regarding population structure, differentiation, and gene flow. We show that there is low genetic differentiation across two prominent geographic breaks and found evidence of recent divergence without subsequent gene flow across them. This pattern supports the hypothesis that currently disjunct patches of dry forest were more connected during the Middle and Late Pleistocene and demonstrates that signatures of this history can be found in the genome of a widespread dry forest bird species.

2 | MATERIALS AND METHODS

2.1 | Sampling

We sampled a total of 90 voucherized museum specimens of *Phacellodomus rufifrons* across virtually its entire range, including all subspecies except *castilloi* from Colombia and Venezuela (see Table S1 for sample details). As outgroups, we sampled its sister species *P. sibilatrix* ($n = 1$) and *P. striaticeps* ($n = 2$). We had particularly thorough sampling of the four southern subspecies that occur along the putative extent of the Pleistocene Arc. After filtering based on DNA quality, read depth, and coverage (see details below), we retained 74 samples of *P. rufifrons* and the three outgroup samples for downstream analyses. Our analyses included individuals from

subspecies *specularis* ($n = 20$), *rufifrons* ($n = 27$), *sincipitalis* ($n = 13$), *peruvianus* ($n = 13$), and *inornatus* ($n = 1$). See below for details on the assignment of individuals to subspecies.

2.2 | mtDNA extraction and sequencing

We extracted total genomic DNA using the E.Z.N.A Tissue DNA Kit (Omega Bio-tek) and PureLink Genomic DNA (Invitrogen Inc.) commercial kits following protocols described by the manufacturers. We amplified the NADH dehydrogenase 2 (ND2; 1,041 base pairs) mitochondrial gene using the protocols described by Brumfield et al. (2007). Cycle-sequencing reactions were conducted using external primers, and sequences were obtained at Eton Biosciences (Cambridge, MA) and the Louisiana State University Genomics Facility.

2.3 | Mitochondrial DNA alignment and haplotype network

Electropherograms were inspected, assembled in contigs, and edited in GENEIOUS v 9.1.5 (Kearse et al., 2012). Clean sequences were aligned using the program Muscle (Edgar, 2004), implemented in Geneious. A sequence of *P. sibilatrix* from GenBank was added to this alignment as an outgroup (Derryberry et al., 2011). Using these ND2 sequences, we constructed a median-joining haplotype network using the program PopART (Bandelt et al., 1999; Leigh & Bryant, 2015).

2.4 | Time-calibrated mitochondrial gene tree

We constructed a time-calibrated mitochondrial gene tree with BEAST v2.4.4 (Bouckaert et al., 2014), with a GTR + Γ substitution model and a strict molecular clock with a rate of 2.1%/Myr (Abadi et al., 2019; Weir & Schluter, 2008). We ran the MCMC for 50,000,000 generations, sampling every 10,000, and used the program TREEANNOTATOR (Drummond & Rambaut, 2007) to generate a maximum clade consensus tree. We assessed convergence (effective sample size values >400) using TRACER 1.7.1 (Rambaut et al., 2018).

2.5 | RADseq sampling, loci assembly and filtering

To sample loci from across the genome, we followed the double-digest Restriction-site Associated DNA sequencing (ddRADseq, hereafter RADseq) protocol developed by Peterson et al. (2012), using the enzymes EcoR1 and SphI. Following library preparation, we sequenced the pooled libraries at the Bauer Core Facility at Harvard University on a standard Illumina HISEQ v4 2 \times 125 bp flowcell.

A total of 215,372,334 125-bp paired-end reads from the Illumina sequencer were imported into the Harvard Odyssey Cluster and processed using the Stacks pipeline (Catchen et al., 2013). See Supporting

information for full details on locus assembly, assembly parameter selection, and filtering. Our final main data set included 77 individuals and 7,167 unlinked SNPs, with missing data parameters set to filter out all loci not found in 60% of individuals (i.e., no more than 40% missing data per locus). We generated four alternative data sets using different combinations of missing data filters, assembly parameters, and forward versus reverse reads (see Supporting information for details). We conducted principal component analyses (PCAs) using ADEGENET v.2.1.1 (Jombart, 2008) implemented in R using each data set, and found that the alternative data sets gave very similar results (Figure S1), so proceeded with our analyses using the primary data set. All individuals were assigned to one of five populations, corresponding to the five described subspecies sampled. This was done using plumage traits, geography and, where subspecies boundaries were not well-defined in the literature, our PCA clusters in conjunction with geography; see Supporting information for full details.

2.6 | Analysis of population structure

We analysed population structuring using STRUCTURE v. 2.3.4 (Pritchard et al., 2000). Because minor alleles that appear only once in the data set have been shown to affect population structure analyses (Linck & Battey, 2019), we filtered out singletons using VCFTOOLS v.0.1.17 (Danecek et al., 2011). After filtering, we ran STRUCTURE with k values between two and six, to capture any potentially hierarchical structuring patterns (Evanno et al., 2005). Each k value was analysed with four independent runs, each with a length of 200,000 and burnin of 50,000 using the default settings. We processed the results using Structure Harvester web v. 0.6.94 (Earl & vonHoldt, 2012) and CLUMPP v. 1.1.2 (Jakobsson & Rosenberg, 2007), and visualized them with DISTRUCT v1.1 (Rosenberg, 2004).

2.7 | Genetic diversity and population differentiation metrics

To evaluate the genetic diversity of each population, we used the program ARLEQUIN v.3.5.2 (Excoffier & Lischer, 2010) for the ND2 data set to calculate nucleotide diversity (π) and Watterson's theta (θ_s), and the populations module of Stacks for the RADseq data set (Catchen et al., 2013) to calculate π .

To measure and compare between-population differentiation, we used Geneious (Kearse et al., 2012), to calculate the minimum, maximum, and mean pairwise distances between all pairs of populations using the ND2 data. We then used the populations module of Stacks to find F_{ST} and F'_{ST} between populations using the RADseq data set.

2.8 | Species tree analysis

We constructed a species tree using SNAPP (Bryant et al., 2012) implemented in BEAST2 (Bouckaert et al., 2014). Because of the

computational and missing data constraints of SNAPP, the two individuals with the lowest percentage of missing data in our primary dataset (7,167 SNPs) were selected from each subspecies or out-group species (two taxa, *iornatus* and *P. sibilatrix*, were represented by one individual), for a total of 12 tips with an average of 12% missing data. Six independent MCMC chains were run for 1,000,000 iterations with default parameters and a burnin of 200,000, sampling every 1,000, following Winger et al. (2015). Chain log files were compiled in LogCOMBINER v.2.4.4 (Bouckaert et al., 2014) and visualized in TRACER v1.7.1 (Rambaut et al., 2018) to check for convergence. Tree files from the independent runs were compiled with LogCOMBINER, a maximum clade credibility tree was generated in TREEANNOTATOR v.2.4.4 (Drummond & Rambaut, 2007), and the sampling of trees from the posterior distribution was visualized in DENSITREE v.2.2.5 (Bouckaert, 2010).

2.9 | Equilibrium patterns of gene flow and genetic diversity

We estimated parameters and tested scenarios associated with equilibrium models of gene flow among the four southern subspecies in a Bayesian framework using MIGRATE-N v. 4.2.14 (Beerli, 2006; Beerli & Felsenstein, 2001). We compared models of panmixia, and two-, three-, and four-populations, with and without symmetrical migration (see Supporting information methods). We ran our migration models using four heated chains, with 10–20 replicates per model to fully explore the parameter space. The results of this were used to compare models using Bayes factor tests based on Bezier-approximated marginal likelihoods (Beerli & Palczewski, 2010). See Supporting information methods for full details on Migrate-n implementation.

2.10 | Demographic analyses using the site-frequency spectra

We used momi2 (Kamm et al., 2019) to conduct demographic history inferences using the joint site-frequency spectra of the four southern populations to evaluate models incorporating population divergence, gene flow, and changes in population size. The simplest null model was built using the well-supported tree topology from the species tree (SNAPP) analyses. The population size of each of the four populations and the timing of the three nodes in the tree were allowed to vary and were optimized using the "L-BFGS-B" algorithm with a maximum of 200 iterations, following the momi2 documentation. This model was optimized over 25 independent runs, and the best performing run (assessed by log-likelihood) was considered to be the optimal parameter set and likelihood value for that model.

We then created alternative models that incorporated gene flow between populations or past changes in population size. To simplify the vast array of possible alternative models, we began by creating 10 simple alternative models (Figure 2a), each of which added

a single additional demographic event to the null model. Four alternative models included a population size change in one of the four populations, with both the magnitude of the change and its timing allowed to vary. The other six alternative models included a single unidirectional migration event moving 10% of individuals from one population to an adjacent population (i.e., *peruvianus* to *sincipitalis* and vice versa, *sincipitalis* to *rufifrons* and vice versa, and *rufifrons* to *specularis* and vice versa). This pulsed migration model as implemented in momi2 may not perfectly reflect the actual demographic history, but rather is a simplified scenario that allows us to test for the presence or absence of post-isolation gene flow. This approach to modelling migration differs from the equilibrium-migration model as implemented in Migrate-n: rather than assuming constant migration rates over time, the pulsed isolation-migration model in momi2 allows for temporal changes in migration rates and for initial divergences between populations. The timing of the migration event was allowed to vary in the optimization. The log-likelihood values of the best performing run of each model were used to generate the AIC value for that model, and models were ranked by AIC.

To test more complex models incorporating multiple demographic events, we took an iterative approach (Blankers et al., 2018; Nater et al., 2015; Pelletier & Carstens, 2014). After ordering all of the simple models by AIC, we combined the two best-performing models and optimized the new two-event model. If this combined

model outperformed all previously tested models, we added in the third-best-performing simple model, and repeated this process until the new combined model did not have a lower AIC value than the previous model. We stopped testing new models when adding an additional demographic event did not improve the AIC score of the model and considered the previous model to be the optimal one. There are some shortcomings of this approach – perhaps some simple models that perform poorly in isolation would improve a combined model more than some models that perform better in isolation – but it gives an empirical framework for testing more complex models, and crucially does not require an *a priori* selection of “likely” complex models.

2.11 | Species distribution modelling

To place our molecular data in a temporal and ecological context, we turned to species distribution modelling (SDM). We used the GBIF (Global Biological Information Facility) database to download a data set of *P. rufifrons* occurrences, to which we added our own sample localities (GBIF, 2016). Because we found the northern populations to be genetically distinct from the others, and outside of the proposed “Pleistocene Arc” region, we focused on only the four southern subspecies for this modelling. Clearly mis-plotted

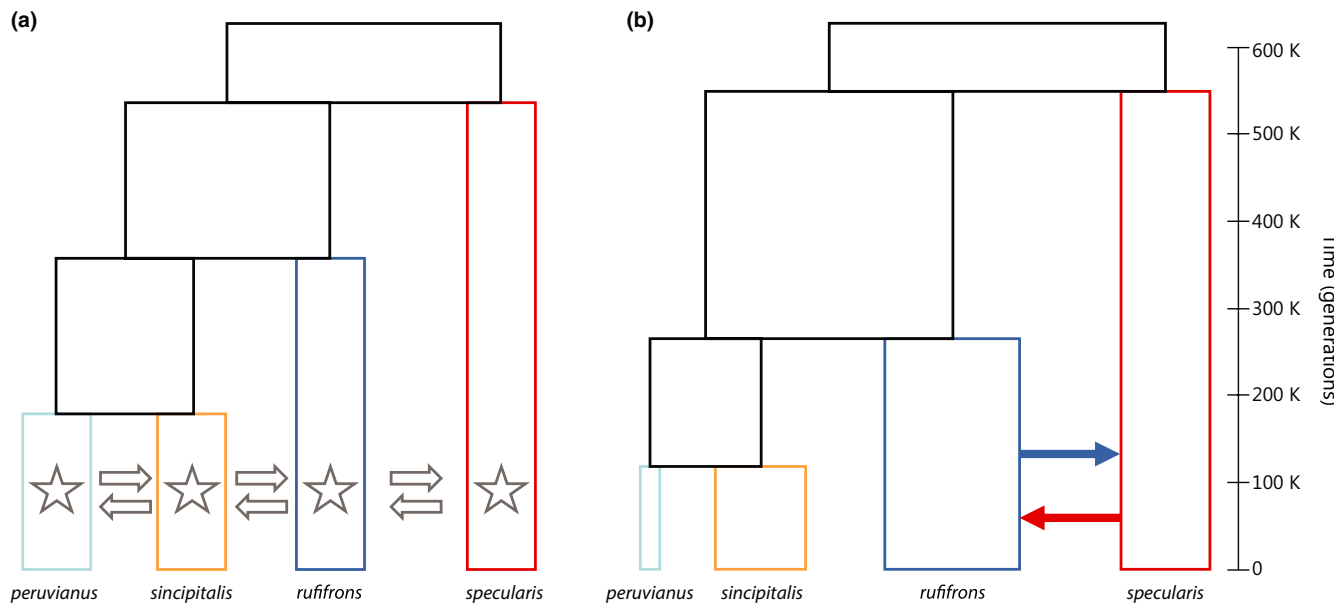


FIGURE 2 (a) Schematic representation of the 11 demographic models tested using the program momi2. The null model is simply the bifurcating tree topology, with population sizes and node ages as the parameters of the model. The 10 alternative models are represented by the six arrows and four stars. Each arrow represents a model that includes a single unidirectional migration event moving 10% of individuals between those two populations – the age of that migration event is an additional parameter of those models. Each star represents a model that allowed for a single change in population size within that population, with the time of the event and the past population size as variable parameters. After testing each of the basic alternative models, the best-performing models were iteratively combined to test more complex models. (b) Graphical representation of the best-supported model from demographic history modeling of southern populations of *P. rufifrons* implemented in momi2. The optimal model included migration events from *rufifrons* to *specularis* and vice versa, but no historical changes in population size. Population sizes of each modern population, timing of all nodes and migration events were allowed to vary, and the optimal parameter values from the best-supported model are represented, with the width of populations proportional to their size (*peruvianus* $n = 166,664$, *sincipitalis* $n = 735,159$, *rufifrons* $n = 1,110,499$, *specularis* $n = 723,140$) and with time in thousands of generations on y-axis. See Table S4 for full parameter details [Colour figure can be viewed at wileyonlinelibrary.com].

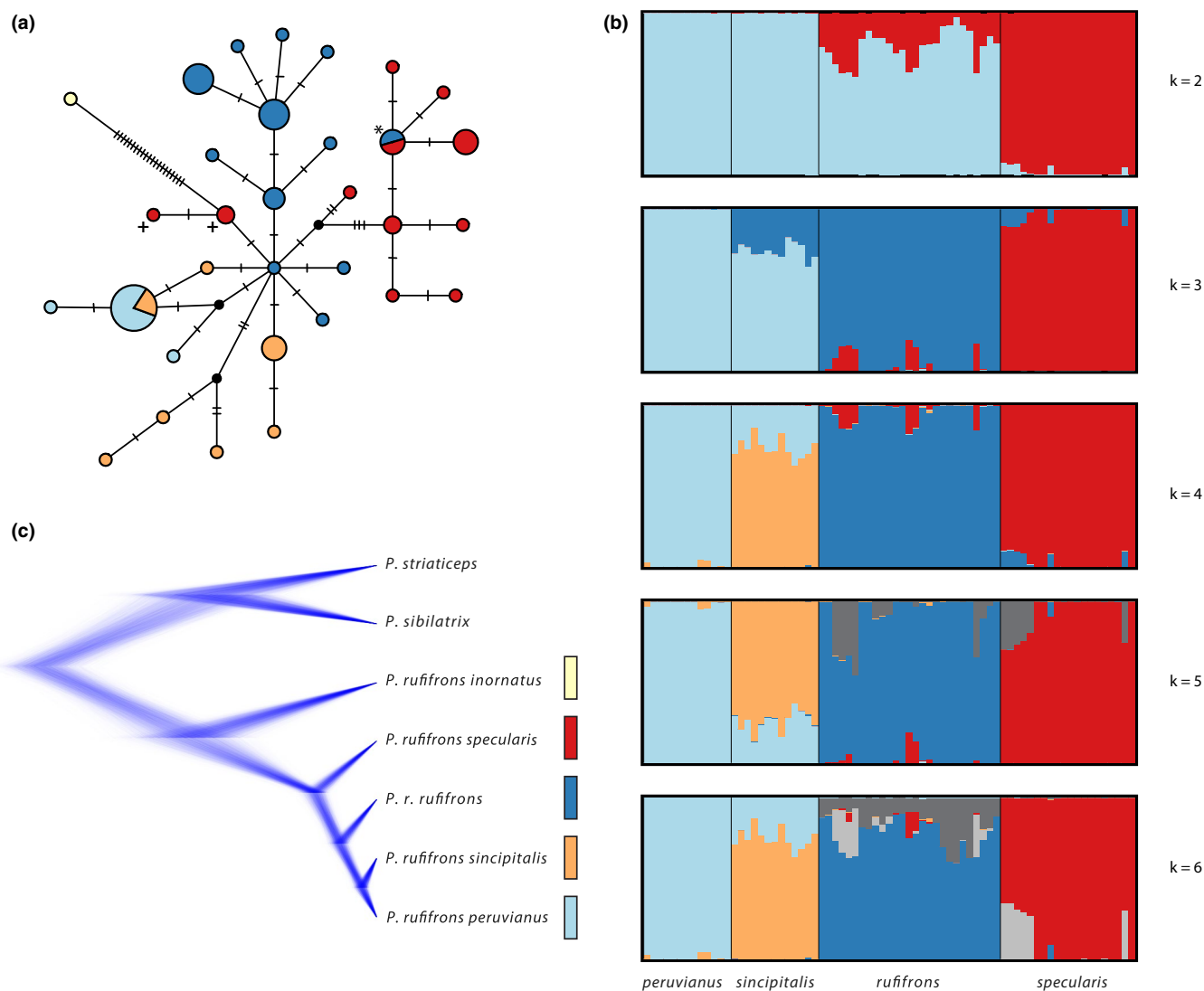


FIGURE 3 Population structure in *P. rufifrons*. Colours correspond to those on the map in Figure 1. (a) Median-joining ND2 haplotype network obtained in PopART. Circles are scaled by the number of individuals sharing that haplotype, and each hash mark between circles represents a single substitution between the haplotypes. Individuals of *rufifrons* with *specularis* mtDNA are marked with *; individuals of *specularis* with *rufifrons* mtDNA are labelled with +. (b) STRUCTURE plots of southern populations of *P. rufifrons* with varying *k* values based on data derived from 7,167 unlinked SNPs obtained via RADseq. Each vertical bar represents an individual. (c) Densitree representation of species trees from the posterior distribution of the SNAPP analysis [Colour figure can be viewed at wileyonlinelibrary.com]

data points, falling well outside the known range of the species, were removed, leaving a total of 1,312 points for the four southern subspecies.

We used the WORLDCLIM v1.4 database to provide the environmental variables for the analysis (Hijmans et al., 2005). We used environmental variable layers at 2.5' resolution from the present day, from a recent warm and dry climate period in the mid-Holocene (~6,000 years before present), and from the Last Glacial Maximum (~21,000 years before present), a cool dry period which Prado and Gibbs (1993) suggest was a period of maximum extent for the dry forest biome. The mid-Holocene and Last Glacial Maximum layers were constructed using the MIROC-ESM paleoclimate model (Hijmans et al., 2005; Watanabe et al., 2011). To avoid using highly correlated variables in the modelling, we conducted a correlation analysis for the 19 bioclimatic variables using ENMtools (Warren et al., 2010)

and selected a single variable from each cluster of correlated variables. Therefore, we used the following six variables: annual mean temperature (Bio1), isothermality (Bio3), temperature seasonality (Bio4), precipitation seasonality (Bio 15), precipitation of the wettest quarter (Bio 16), and precipitation of the driest quarter (Bio 17). None of the variables had correlation coefficients greater than 0.7 with any of the other variables used. Variables were clipped to encompass solely South America using QGIS v3.6 (QGIS Development Team, 2017).

We created species distribution models using Maxent (Phillips et al., 2006), which automatically eliminates multiple sightings from the same grid square in the environmental variable layers, leaving 480 distinct localities. Taking advantage of the large number of available points, models were constructed using subsampling of 50% of the points to serve as test points during each replicate. Each model

was run with 10 subsampling replicates. All models were visualized using QGIS (QGIS Development Team, 2017).

3 | RESULTS

3.1 | Mitochondrial DNA

A median-joining haplotype network of the ND2 samples (Figure 3a) shows that the northern subspecies *inornatus* is distinct from the remaining individuals (2.11% minimum uncorrected sequence divergence), but there is little mitochondrial differentiation among the southern subspecies. For instance, the most common *peruvianus* ND2 haplotype is shared with *sincipitalis*. The majority of *specularis* samples cluster apart from *rufifrons*, but there are exceptions. Two individuals from Bahia assigned to *rufifrons* using the RADseq data (marked on the network in Figure 3a with “*”) cluster with *specularis*, and even share a haplotype with two *specularis* individuals. Similarly, three individuals with *specularis* nuclear genomes (Figure 3a, indicated with “+”) from Pernambuco and Alagoas cluster with the *rufifrons* ND2 haplotypes.

A time-calibrated ND2 Bayesian tree (Figure S2) shows a similar pattern: although the *inornatus* sample is highly distinct, there is low support for most nodes within the southern clade. According to our time-calibrated tree, *P. rufifrons* diverged from *P. sibilatrix* between 1.67 and 3.06 million years ago (Ma), and the southern *P. rufifrons* populations diverged from *inornatus* between 0.82 and 1.75 Ma. Because none of the southern subspecies are monophyletic in the mtDNA tree, we cannot easily estimate divergences between each of them, but the crown age of the southern clade is between 240,000 and 560,000 years, corresponding to the Middle Pleistocene.

3.2 | RADseq analyses of population structure and phylogeny

A total of 199,768,488 raw reads were successfully demultiplexed and assigned to 86 individuals. This resulted in an average of 2,322,889 reads per individual prior to filtering out of nine low-coverage individuals, and 2,546,724 reads per individual after filtering to 77 individuals. Filtering also raised the average coverage depth per individual from 32.1 \times to 34.8 \times . The final product of the stacks pipeline was a data set of 7,167 putatively unlinked SNPs, each of which was present in more than 60% of the 77 selected individuals. The mean percentage of the total loci present in each individual was 76.6%, which corresponds to an average of 5,488 SNPs per individual.

Our STRUCTURE analysis, using a series of k values from 2 to 6, showed deep structure between *specularis* and the remaining southern populations, and a close grouping between *sincipitalis* and *peruvianus* (Figure 3b). At $k = 2$, the individuals are divided into a northeastern Brazilian *specularis* group and a group containing all remaining samples. A substantial proportion of each *rufifrons* sample

TABLE 1 Measures of genetic diversity for southern populations of *Phacelodomus rufifrons*

Population	ND2 θ per site π	ND2 θ s per site	RADseq π
<i>peruvianus</i>	0.00045	0.00100	0.063
<i>sincipitalis</i>	0.00359	0.00386	0.082
<i>rufifrons</i>	0.00265	0.00407	0.092
<i>specularis</i>	0.00357	0.00426	0.088

is assigned to the *specularis* population. At $k = 3$, *peruvianus*, *rufifrons*, and *specularis* each form a cluster, with a low level of potential admixture between *rufifrons* and *specularis*. Although the *sincipitalis* individuals are each assigned largely to the *peruvianus* group, approximately a quarter of each individual corresponds to the *rufifrons* group. At $k = 4$, which is the “optimal” number of clusters according to the Evanno method (Evanno et al., 2005), each subspecies is assigned its own cluster, though an average of 26% of each *sincipitalis* individual continues to be assigned to the *peruvianus* cluster, and there are much smaller proportions of *specularis* and *rufifrons* individuals assigned to the other’s clusters. At $k = 5$ and $k = 6$ the plot is essentially unchanged, with the additional clusters accounting only for a small proportion of a few individuals, with no apparent geographic pattern.

In our Bayesian SNAPP tree (Figure 3c), *P. rufifrons* is sister to the clade of *P. sibilatrix* and *P. striaticeps*. Within *P. rufifrons*, *inornatus* is sister to a clade formed by all southern subspecies. Within this southern clade, *specularis* is sister to the rest, and *rufifrons* in turn is sister to a clade comprising *peruvianus* and *sincipitalis*. This topology is fully supported at all nodes and corresponds to the STRUCTURE results as k increases. In the SNAPP tree the relative age of the split between *inornatus* and the southern subspecies is roughly equivalent to the age of the split between *P. sibilatrix* and *P. striaticeps*.

3.3 | Population diversity and differentiation statistics

We obtained measures of genetic diversity and population differentiation based on both mtDNA and RADseq data (Tables 1 and 2). For all three measures of diversity used (ND2 π , ND2 θ , and RADseq π), *peruvianus* had substantially lower genetic diversity than the remaining three southern populations.

The uncorrected ND2 sequence divergences are all much higher between *inornatus* and the southern subspecies than among the southern subspecies (Table 2). The minimum sequence divergence between *inornatus* and any of the southern individuals is 2.11%, whereas no pairs of southern populations have a minimum divergence above 0.3% or a maximum divergence above 1%. Among the southern populations, the mean and maximum divergences between pairs of populations generally correspond to the phylogeny, with the lowest values between *peruvianus* and *sincipitalis* and the highest between *specularis* and the rest. This pattern

TABLE 2 Pairwise population genetic differentiation within *Phacelodromus rufifrons*

Pairing	Avg. ND2 unc. seq. divergence (%) (min–max)	RADseq F_{ST}	RADseq F'_{ST}
<i>inornatus</i> – <i>peruvianus</i>	2.43 (2.4–2.5)	0.33	0.51
<i>inornatus</i> – <i>sincipitalis</i>	2.41 (2.21–2.62)	0.21	0.39
<i>inornatus</i> – <i>rufifrons</i>	2.33 (2.21–2.69)	0.13	0.32
<i>inornatus</i> – <i>specularis</i>	2.57 (2.11–2.79)	0.15	0.34
<i>peruvianus</i> – <i>sincipitalis</i>	0.30 (0–0.68)	0.08	0.11
<i>peruvianus</i> – <i>rufifrons</i>	0.43 (0.19–0.77)	0.07	0.15
<i>peruvianus</i> – <i>specularis</i>	0.64 (0.29–0.87)	0.12	0.24
<i>sincipitalis</i> – <i>rufifrons</i>	0.44 (0.1–0.88)	0.05	0.09
<i>sincipitalis</i> – <i>specularis</i>	0.64 (0.19–0.97)	0.09	0.18
<i>rufifrons</i> – <i>specularis</i>	0.60 (0–0.87)	0.06	0.11

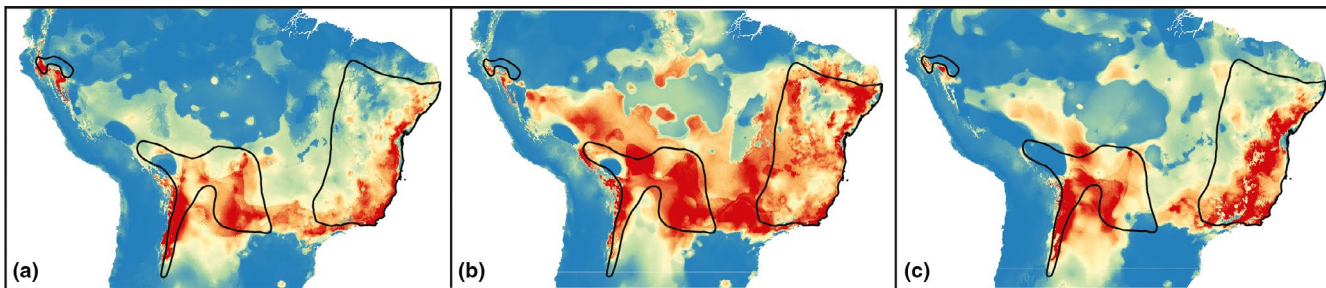


FIGURE 4 Species distribution modelling through time implemented in Maxent. (a) Inferred distribution for the present day; (b) mid-Holocene, 6 ka; and (c) Last Glacial Maximum, 21 ka. Warmer colours indicate greater probability of occurrence. Models for the LGM and mid-Holocene were based on the MIROC-ESM climate model. Black outlines represent the current range of the southern subspecies of *P. rufifrons*, per Birdlife International [Colour figure can be viewed at wileyonlinelibrary.com]

breaks down when looking at the minimum divergences, because two pairs of populations share haplotypes (*peruvianus*/*sincipitalis* and *rufifrons*/*specularis*).

The RADseq F_{ST} and F'_{ST} results are similar to the pattern shown by the mean ND2 divergences – high values between *inornatus* and the others, and lower values among the southern populations (Table 2). The F_{ST} and F'_{ST} values between *sincipitalis* and *rufifrons* are particularly low, and the F_{ST} and F'_{ST} comparisons between *specularis* and *rufifrons* are lower than between *specularis* and the other two southern subspecies.

3.4 | Analyses of demographic history

Comparison of five equilibrium migration models involving symmetrical and unconstrained gene flow was conducted using Migrate-n. All models involving migration assumed a stepping-stone model in which no gene flow occurred between nonadjacent populations. Bayes factor comparison of models overwhelmingly supported the most complex model, with each of the four southern subspecies as a distinct population and variable rates of bidirectional gene flow between them (Table S2). Estimates of gene flow were generally quite high, corresponding to 9.6–13.1 migrants per generation between populations (Table S3). In the 4-population symmetrical migration

model, the highest migration rates were estimated between *rufifrons* and *specularis*, whereas in the full model, the highest average rates between *peruvianus* and *sincipitalis* (11.4) were slightly higher than between *rufifrons* and *specularis* (10.9). Estimates of θ for each population were very uniform but were probably dominated by the prior in this version of migrate (P. Beerli, personal communication).

We next tested hypotheses of the demographic history of the southern subspecies in the program momi2 without assuming an equilibrium model. Instead, our momi2 models assumed a well-supported branching topology (as in Figure 3c). Of the null model and the first set of alternate models (see Table S4), the best-performing model involved migration from *rufifrons* to *specularis*, and the second-best model involved migration from *specularis* to *rufifrons*. These two models were combined, and the resulting model, with migration events in both directions between *rufifrons* and *specularis*, outperformed all of the first set of alternative models (Figure 2b). However, when the third best-supported event was added as well – a change in the population size of *sincipitalis* – the new model did not outperform the model with just the two migration events. These results are similar to those of the 4-population symmetrical migration results from Migrate in supporting high gene flow between the divergent, but parapatric, *rufifrons* and *specularis*, but suggest that population size changes or migration between *peruvianus*, *specularis*, and *rufifrons* are not necessary to explain the data.

3.5 | Species distribution modelling

We used species distribution modelling to predict the expected distribution of the southern populations of *P. rufifrons* at the Last Glacial Maximum, a cool dry period c. 21 ka, and the Mid-Holocene, a warm dry period c. 6 ka (Figure 4). The present-day model ($AUC = 0.906$) closely mirrored the current distribution of the species, albeit with some over-representation in former Atlantic Forest regions of coastal Brazil that are now pastureland more suitable for the species, and some underrepresentation in sparsely sampled interior regions of the Caatinga. Compared to the present-day model, both the mid-Holocene and LGM models ($AUC = 0.905$ for both) predict greater habitat suitability in southern and central Peru between the modern ranges of *peruvianus* and *sincipitalis*. In the mid-Holocene, but not the LGM, the model also predicts greater habitat suitability in southwestern Brazil, between the present-day distributions of *sincipitalis* and *rufifrons*. Overall, the historical models suggest a more contiguous distribution of the species in the recent past, particularly between *peruvianus* in Peru and *sincipitalis* in Bolivia.

4 | DISCUSSION

Our results shed light on three distinct biogeographic, evolutionary, and taxonomic questions involving *P. rufifrons* and the Neotropical dry forest biome in general. First, and most significantly, we found evidence that populations of *P. rufifrons* in currently disjunct patches of dry forest were connected in the recent past, the pattern predicted by the Pleistocene Arc Hypothesis. Second, we found a relatively deep divergence with recent gene flow between parapatric populations in eastern Brazil, indicating an apparent zone of secondary contact between previously isolated populations. Finally, our results were consistent (albeit with limited sampling) with the treatment of the northern *inornatus* group as a species-level taxon.

4.1 | Evidence for the Pleistocene Arc Hypothesis

The primary impetus for this study was to test the Pleistocene Arc Hypothesis by using genomic data to examine the phylogeographic relationships and demographic history of *P. rufifrons*. In doing so, we attempted to distinguish between the Pleistocene Arc model and two potential alternative hypotheses: (i) that disjunct *P. rufifrons* populations diverged prior to the Pleistocene, precluding a role for recent Quaternary climate fluctuations in their divergence; or (ii) that there have not been significant changes in *P. rufifrons* habitat connectivity over time, and that long-distance dispersal is responsible for its present-day distribution. We found little genetic differentiation between highly geographically disjunct populations – *peruvianus*, *sincipitalis*, and *rufifrons* – indicating recent divergence times. Furthermore, we showed that the relative degree of geographic disjunction between present-day southern *P. rufifrons* populations does not correspond to their relative degree of genetic differentiation,

as might be expected in a dispersal-only model. In fact, the highly disjunct *peruvianus* and *sincipitalis* subspecies are the most closely related, whereas the parapatric *rufifrons* and *specularis* subspecies are the most distant, albeit with signals of recent gene flow. This pattern demonstrates that the genetic structuring of this species was probably established when its distribution was dramatically different from today.

The relationship between *peruvianus* and *sincipitalis* is emblematic of this pattern: they are separated by more than 1,000 km of rainforest habitat highly unsuitable for this species, yet are sister populations and share mitochondrial haplotypes. At lower values of k in our STRUCTURE analysis these two populations are considered a single cluster, and even at higher values of k a proportion of each *sincipitalis* individual is assigned to the *peruvianus* cluster. Though this provides clear evidence for a close relationship between *sincipitalis* and *peruvianus*, it is unlikely that there has been pervasive gene flow from the much smaller *peruvianus* population across the entirety of the larger *sincipitalis* population, with no admixture in the opposite direction. It is more probable that this is a case in which a small population (*peruvianus*) registers as quite distinct to the STRUCTURE algorithm, and “pulls” a proportion of the individuals in its sister or parental population (*sincipitalis*) with it, as shown in recent simulations (Lawson et al., 2018). Analysis of demographic history using momi2 does not support a post-dispersal bottleneck in *peruvianus*, as would be expected if the population was founded by a long-distance dispersal event from the *sincipitalis* population. Additionally, if the intervening rainforest is a lesser barrier to dispersal in *P. rufifrons* than is generally believed, we would expect there to be occasional dispersal events and evidence for ongoing gene flow between the populations, which is not supported by our momi2 analysis. Although our Migrate-n results do suggest high estimates of equilibrium gene flow (Table S3), this appears to be a function of Migrate-n assuming an equilibrium migration model, rather than a tree-like isolation model, and thus interpreting shared polymorphisms between populations as gene flow. In this system, where we have shown that divergences between populations are recent, the isolation-migration model as implemented in momi2 probably better reflects the true demographic history.

On the whole, the most likely scenario is that *peruvianus* and *sincipitalis* were connected through formerly suitable habitat in central and southern Peru in the recent past, and that the large modern-day disjunction between them is a recent phenomenon. This scenario is consistent with our species distribution modelling, which predicts substantially increased suitability for *P. rufifrons* in the region during both the mid-Holocene and the LGM. Given this prediction of expanded range size for *P. rufifrons* under past climatic regimes, it is somewhat surprising that our momi2 results did not support models with changes in population size for any of the subspecies. However, our relatively simple demographic models may not have had the resolution to identify repeated cyclical fluctuations in population size. Our proposed scenario is also consistent with the predictions of other previously published species distribution models, which similarly show increased

dry forest habitat suitability along the southwest fringe of the Amazon during Late Pleistocene dry periods (Savit & Bates, 2015; Werneck et al., 2011, 2012). This region, where today the Amazon meets the Andes, should be a central focus of future tests of the Pleistocene Arc Hypothesis. Indeed, the prospect of a historical "Andean corridor" that once connected the dry forest birds of northern Peru with those of Bolivia and Brazil was put forward by Haffer (1967). This model has been considered secondary to other potential cross-Amazonian dispersal routes for savanna birds and rattlesnakes, but has not been investigated in depth for dry forest species (Quijada-Mascareñas et al., 2007; Silva & Bates, 2002).

As with *peruvianus* and *sincipitalis*, there is a pattern of low genetic differentiation across a large range disjunction when comparing *sincipitalis* and *rufifrons*, which have the lowest nuclear F_{ST} and F'_{ST} of any pair of populations, and which contain individuals that differ from each other by only a single ND2 nucleotide substitution. They are separated by a 500 km range break, although the intervening Cerrado habitat is probably a weaker barrier to *P. rufifrons* dispersal than the rainforest separating *peruvianus* and *sincipitalis*, and anthropogenic habitat change may be eroding this gap. Our estimates of divergence time using momi2 put the *specularis*-*rufifrons* split in the Middle Pleistocene, within the period of frequent glacial and interglacial cycles. This is, however, substantially earlier than the split between *peruvianus* and *sincipitalis*, suggesting that different patches of dry forest along the Pleistocene Arc became isolated asynchronously. Our SDMs are less informative in this case because of the complexities of modelling the distinction between dry forest and savanna, which is influenced to a large degree by soil composition, elevation, and fire regimes in addition to precipitation and other climate variables (Collevatti et al., 2013; Särkinen et al., 2011). Regardless, it is apparent from the phylogenetic proximity of the two populations that their divergence is relatively recent and was probably driven by Pleistocene climate fluctuations.

A number of species from many groups of organisms share similar distributions to that of *P. rufifrons* (Mogni et al., 2015; Pennington et al., 2000; Prado, 1991; Prado & Gibbs, 1993). In birds, many widespread dry forest species show the same pattern of highly disjunct populations in the dry Marañon, Huallaga, or Mayo valleys of northern Peru (Vásquez et al., 2018) (see Table S5 for a list of species). Some, like *P. rufifrons*, have entirely disjunct ranges between the northern Peruvian valleys and Bolivia, but others have additional isolated populations in dry pockets further south along the extent of the proposed dry forest arc between northern Peru and Bolivia, such as the Urubamba Valley and Gran Pajonal (see Table S5) (Chapman, 1921; Harvey et al., 2011; Vásquez et al., 2018). If the pattern seen in *P. rufifrons* holds, then the northern Peruvian populations of these species would have diverged recently from closely related populations in Bolivia, with isolated populations in open dry habitats in central Peru perhaps representing additional remnants of previously more extensive dry forest in this region (Chapman, 1921; Haffer, 1967; Linares-Palomino, 2006).

Of course, differential dispersal can produce idiosyncratic species-specific responses to the same geographic barrier, as shown

in comparative phylogeographic studies (Naka & Brumfield, 2018; Smith et al., 2014), including in dry forest birds (Oswald et al., 2017). Additionally, different dry forest species will vary in their ability to inhabit a range of suboptimal habitats. Thus, fluctuating levels of habitat suitability between disjunct dry forest patches may have presented varyingly permeable barriers to species of differing dispersal abilities at different points in time. The hand-wing index of *P. rufifrons* – a metric of wing roundness in which lower numbers are used as a proxy for lower flight efficiency and dispersal ability (Baldwin et al., 2010; Burney & Brumfield, 2009; Claramunt et al., 2012; Dawideit et al., 2009; Kipp, 1959; Sheard et al., 2020) – was measured as 13.6 in one study, putting it in the 36th percentile within its largely sedentary family (Claramunt et al., 2012). A second study obtained a similarly low hand-wing index value of 13.15 for *P. rufifrons*, which puts it in only the 17th percentile in their data set of nearly all bird species (Sheard et al., 2020). By contrast, dry forest bird species with similar disjunct distribution patterns include species with pointed wings and high flight performance, like the Planalto Hermit (*Phaethornis pretrei*), and partially migratory species such as the Red-crested Finch (*Coryphospingus cucullatus*). Comparative phylogeographic work on a range of species (such as those listed in Table S5) would give insight into the relative influence of overarching climatic processes compared to species-specific traits in generating patterns of genetic structure in dry forest birds.

4.2 | Secondary contact with gene flow between Brazilian subspecies

A second significant finding of this study is the complex relationship between the parapatric subspecies *rufifrons* and *specularis* in eastern Brazil. The northeastern subspecies *specularis* has been recognized as being morphologically distinct due to its reddish primary patch, which is not found in *rufifrons* or any other subspecies (Remsen, 2003a; Ridgely & Tudor, 2009). However, the exact boundary between the two subspecies, including whether there is a sharp morphological break or a plumage cline, remains to be studied. We found that *specularis* is the most genetically distinct among the southern subspecies of *P. rufifrons* and is sister to the three other southern subspecies. This pattern was unanticipated because, unlike the other southern subspecies, *specularis* and *rufifrons* are parapatric and the boundary between them does not seem to correspond to any known current or past biogeographic barrier. Near the coast the break may be close to the São Francisco River, but this relationship does not hold in the interior, with multiple *rufifrons* individuals found on the left bank of the river in Bahia, Tocantins, and southern Piauí. The range of *specularis* encompasses more arid Caatinga habitats than that of *rufifrons*, a promising avenue for research in dry forest birds (Termignoni-García et al., 2017). Breaks between genetic clusters have been found in similar locations in a plant (Caetano et al., 2008) and a lizard (Werneck et al., 2012), and were proposed to correspond to an ecological transition between true Caatinga and more Cerrado-like habitats (Werneck et al., 2012).

Despite the comparatively deep divergence between *rufifrons* and *specularis*, we found evidence of gene flow between the subspecies, including individuals in Bahia, Alagoas, and Pernambuco which were assigned to one population using genomic data, but which shared ND2 haplotypes with individuals of the other subspecies. This is supported by our demographic history analysis, which found strong support for a model of early divergence and recent gene flow between the two populations, and by the lower values of F_{ST} and F'_{ST} between *specularis* and *rufifrons* than between *specularis* and the other southern subspecies. Because hybrid zones are ideal “natural laboratories” to study evolutionary processes (Hewitt, 1988; Price, 2008), this previously unrecognized contact zone warrants substantial further sampling and investigation, with a focus on determining the position and nature of genetic and morphological breaks, and whether they correspond to geographic or ecological barriers. Additionally, in suboscines like *P. rufifrons*, vocal differences are considered of central importance in promoting reproductive isolation (Isler et al., 1998, 2005; Remsen, 2005; Seddon & Tobias, 2007; Tobias et al., 2012), but lack of clarity over the geographic boundaries between the subspecies has impeded work on differentiating the vocalizations of *rufifrons* and *specularis* (Boesman, 2016). Detailed vocal, morphological, and genetic data at a fine geographic scale will be needed to illuminate the evolutionary dynamics at work in this putative contact zone.

4.3 | Taxonomic status of northern subspecies

Finally, our genetic data is relevant to the question of species limits within the Rufous-fronted Thornbird. Although the northern two subspecies, *inornatus* and *castilloi*, have been considered by some authorities to represent a distinct species, *P. inornatus*, on the basis of plumage and vocal differences (Boesman, 2016; Hilty, 2003; del Hoyo et al., 2017; Ridgely & Tudor, 2009), this treatment is not universal (Dickinson & Christidis, 2014; Remsen, 2003b). Our single *inornatus* sample is insufficient to draw any absolute conclusions on this subject. However, that sample was clearly more distinct (>2% ND2 sequence divergence) from the southern samples than any of the southern samples were from each other. The *inornatus* individual was sister to the southern subspecies in all phylogenetic trees that we inferred, and the age of this split was more similar to that between *Phacellodomus sibilatrix* and *P. striaticeps*, which are unambiguously regarded as distinct species, than to the age of any other split within *P. rufifrons*. Therefore, the preliminary genetic evidence provided here is consistent with the treatment of *P. inornatus* as a species-level taxon. Unfortunately, *P. r. castilloi* was not sampled in this study, but all previous authors have considered it closely related to *inornatus*, and it would presumably be part of the *inornatus* group (Boesman, 2016; del Hoyo, et al., 2017; Ridgely & Tudor, 2009). Further sampling of both *castilloi* and *inornatus* would be crucial to definitively resolving the appropriate treatment of these taxa, as would further study of the proposed vocal differences. This question bears some relevance to the Pleistocene Arc Hypothesis,

because *inornatus* and *castilloi* are the only subspecies that are not found in regions originally proposed as part of the Pleistocene Arc, and are not predicted by our SDMs to have been connected to the other subspecies during the Pleistocene. In fact, if those two subspecies are split off as *P. inornatus*, then the range of remaining *P. rufifrons* sensu stricto will be in near-perfect correspondence with the Pleistocene Arc as proposed by Prado and Gibbs, making it an archetypical example of this distribution pattern in birds.

In conclusion, our work provides one of the first examples of a genome-wide data set that shows the role of Pleistocene climate fluctuations in promoting past connections between currently disjunct dry forest populations. As next-generation sequencing techniques are brought to bear on a wider variety of taxa, we will be able to determine the degree to which other dry forest species show similar genomic signatures of these connections in the recent past, giving us a greater understanding of the evolutionary history of this unique biome and the species that inhabit it.

ACKNOWLEDGEMENTS

For loan of tissues, we thank the Museu de Zoologia da Universidade de São Paulo (MZUSP), Louisiana State University Museum of Natural Science (LSUMZ), the University of Kansas Natural History Museum (KU), the Florida Museum of Natural History (UF), the American Museum of Natural History (AMNH), and the Field Museum of Natural History (FMNH). We are indebted to M. Lima and M. Félix for their assistance with specimen preparation at MZUSP. We thank A. De Luca, J. M. Ferreira, V. Piacentini, T. Pongiluppi, M. A. Rego, M. Somenzari for assistance in the field, and J. M. Ferreira and V. Piacentini for having made field expeditions possible. We thank many current and past members of the Edwards Laboratory for methodological assistance, including A. Shultz, S. Sin, T. Sackson, F. Termignoni Garcia, A. Cloutier, K. Näpflin, J. Schmitt, P. Grayson, S. Lamichhaney, and J. Burley. For aid in the original development of the project we thank the members of the Laboratory of Avian Ecology & Evolution at the Federal University of Pernambuco in Brazil, including D. Mariz, J. Ramos, S. Menezes, and L. Viturino de Freitas. We thank J. Battilana, S. Herke, A. Gouvêa, and D. Cueva for their assistance with laboratory work, and B. Ehlers and W.L. de Moreas Neto for support in field and laboratory work. We also thank P. Beerli and G. Del-Rio for their guidance on genomic analyses. We thank J.V. Remsen Jr., F. Werneck, and two anonymous reviewers for their helpful comments on the manuscript. Figures were constructed with the help of visuals from Birdlife International, T. Särkinen, and especially T. Worfolk and the team of the Handbook of the Birds of the World at Lynx Edicions. Laboratory work was conducted with the help of the FAS Bauer Core Facility at Harvard University, the Molecular Biology Laboratory at the Museu de Zoologia da Universidade de São Paulo, and the Louisiana State University Genomics Facility. Analyses were run using the Odyssey Cluster supported by the Harvard University FAS Research Computing Group. Financial support was provided by the Museum of Comparative Zoology Grants-in-aid of Undergraduate Research (to

ECC), the Harvard University Center for the Environment Summer Research Fund (to ECC), the Harvard College Research Program (to ECC), the São Paulo Research Foundation – FAPESP (2012-23852-0 to GAB; 2018/20249-7 and 2017/23548-2 to LFS), the Pernambuco Research Foundation – FACEPE (APQ-0337-2.04/15 to LNN), the Brazilian Research Council – CNPq (457974-2014-1 to GAB and LFS; 302291/2015-6 and 308337/2019-0 to LFS, and 432630/2016-3 to LNN), and the National Science Foundation – NSF (DEB 1831560 to SVE).

AUTHOR CONTRIBUTIONS

All authors conceived the study; E.C.C., G.A.B., S.V.E., F.S., and L.N.N. designed the research; F.S., E.C.C., and G.A.B. gathered the data; E.C.C., G.A.B., and S.V.E. analysed the data; G.A.B., and E.C.C. constructed figures; E.C.C. wrote the manuscript with input from G.A.B., S.V.E., L.N.N., F.S., and L.F.S.

DATA ACCESSIBILITY

Mitochondrial DNA sequences produced for this study are deposited in GenBank (Accession numbers MT977542 - MT977625), and Illumina reads in the NCBI Sequence Read Archive (BioProject accession number PRJNA662342). Assembled SNP files, scripts, and other data are deposited at Github (<https://github.com/eamonccorbett/phacelodomus>).

ORCID

Eamon C. Corbett  <https://orcid.org/0000-0002-1363-813X>
 Gustavo A. Bravo  <https://orcid.org/0000-0001-5889-2767>
 Fabio Schunck  <https://orcid.org/0000-0002-0974-2655>
 Luciano N. Naka  <https://orcid.org/0000-0002-7716-3401>
 Luís F. Silveira  <https://orcid.org/0000-0003-2576-7657>
 Scott V. Edwards  <https://orcid.org/0000-0003-2535-6217>

REFERENCES

Ab'Saber, A. N. (1977). Espaços ocupados pela expansão dos climas secos na América do Sul, por ocasião dos períodos glaciais quaternários. *Paleoclimas*, 3, 1-19.

Abadi, S., Azouri, D., Pupko, T., & Mayrose, I. (2019). Model selection may not be a mandatory step for phylogeny reconstruction. *Nature Communications*, 10(1), 934. <https://doi.org/10.1038/s41467-019-10822-w>

Arruda, D. M., Schaefer, C. E. G. R., Fonseca, R. S., Solar, R. R. C., & Fernandes-Filho, E. I. (2018). Vegetation cover of Brazil in the last 21 ka: New insights into the Amazonian refugia and Pleistocene arc hypotheses. *Global Ecology and Biogeography*, 27(1), 47-56. <https://doi.org/10.1111/geb.12646>

Avise, J. C., & Walker, D. E. (1998). Pleistocene phylogeographic effects on avian populations and the speciation process. *Proceedings of the Royal Society of London. Series B: Biological Sciences*, 265(1395), 457-463. <https://doi.org/10.1098/rspb.1998.0317>

Baker, P. A., Fritz, S. C., Battisti, D. S., Dick, C. W., Vargas, O. M., Asner, G. P., & Prates, I. (2020). Beyond Refugia: New insights on quaternary climate variation and the evolution of biotic diversity in tropical South America. In V. Rull, & A. C. Carnaval (Eds.), *Neotropical diversification: Patterns and processes* (pp. 51-70). Springer International Publishing. https://doi.org/10.1007/978-3-030-31167-4_3

Baldwin, M. W., Winkler, H., Organ, C. L., & Helm, B. (2010). Wing pointedness associated with migratory distance in common-garden and comparative studies of stonechats (*Saxicola torquata*). *Journal of Evolutionary Biology*, 23(5), 1050-1063. <https://doi.org/10.1111/j.1420-9101.2010.01975.x>

Bandelt, H. J., Forster, P., & Röhl, A. (1999). Median-joining networks for inferring intraspecific phylogenies. *Molecular Biology and Evolution*, 16(1), 37-48. <https://doi.org/10.1093/oxfordjournals.molbev.a026036>

Beerli, P. (2006). Comparison of Bayesian and maximum-likelihood inference of population genetic parameters. *Bioinformatics*, 22(3), 341-345. <https://doi.org/10.1093/bioinformatics/bti803>

Beerli, P., & Felsenstein, J. (2001). Maximum likelihood estimation of a migration matrix and effective population sizes in n subpopulations by using a coalescent approach. *Proceedings of the National Academy of Sciences*, 98(8), 4563-4568. <https://doi.org/10.1073/pnas.081068098>

Beerli, P., & Palczewski, M. (2010). Unified framework to evaluate panmixia and migration direction among multiple sampling locations. *Genetics*, 185(1), 313-326. <https://doi.org/10.1534/genetics.109.112532>

Behling, H. (1998). Late quaternary vegetational and climatic changes in Brazil. *Review of Palaeobotany and Palynology*, 99(2), 143-156. [https://doi.org/10.1016/S0034-6667\(97\)00044-4](https://doi.org/10.1016/S0034-6667(97)00044-4)

Blankers, T., Vilaça, S. T., Waurick, I., Gray, D. A., Hennig, R. M., Mazzoni, C. J., Mayer, F., & Berdan, E. L. (2018). Demography and selection shape transcriptomic divergence in field crickets. *Evolution*, 72(3), 553-567. <https://doi.org/10.1111/evol.13435>

Boesman, P. (2016). Notes on the vocalizations of Rufous-fronted Thornbird (*Phacellodomus rufifrons*). HBW Alive Ornithological Note 95. In J. del Hoyo, A. Elliott, J. Sargatal, D. A. Christie, & E. de Juana (Eds.), *Handbook of the birds of the world alive*. Lynx Ediciones.

Bouckaert, R. (2010). DensiTree: Making sense of sets of phylogenetic trees. *Bioinformatics*, 26(10), 1372-1373. <https://doi.org/10.1093/bioinformatics/btq110>

Bouckaert, R., Heled, J., Kühnert, D., Vaughan, T., Wu, C.-H., Xie, D., Suchard, M. A., Rambaut, A., & Drummond, A. J. (2014). BEAST 2: A software platform for bayesian evolutionary analysis. *PLOS Computational Biology*, 10(4), e1003537. <https://doi.org/10.1371/journal.pcbi.1003537>

Brumfield, R. T., Tello, J. G., Cheviron, Z. A., Carling, M. D., Crochet, N., & Rosenberg, K. V. (2007). Phylogenetic conservatism and antiquity of a tropical specialization: Army-ant-following in the typical antbirds (Thamnophilidae). *Molecular Phylogenetics and Evolution*, 45(1), 1-13. <https://doi.org/10.1016/j.ympev.2007.07.019>

Bryant, D., Bouckaert, R., Felsenstein, J., Rosenberg, N. A., & RoyChoudhury, A. (2012). Inferring species trees directly from biallelic genetic markers: bypassing gene trees in a full coalescent analysis. *Molecular Biology and Evolution*, 29(8), 1917-1932. <https://doi.org/10.1093/molbev/mss086>

Burke, K. D., Williams, J. W., Chandler, M. A., Haywood, A. M., Lunt, D. J., & Otto-Bliesner, B. L. (2018). Pliocene and Eocene provide best analogs for near-future climates. *Proceedings of the National Academy of Sciences*, 115(52), 13288-13293. <https://doi.org/10.1073/pnas.1809600115>

Burney, C. W., & Brumfield, R. T. (2009). Ecology predicts levels of genetic differentiation in Neotropical birds. *The American Naturalist*, 174(3), 358-368. <https://doi.org/10.1086/603613>

Caetano, S., Prado, D., Pennington, R. T., Beck, S., Oliveira-Filho, A., Spichiger, R., & Naciri, Y. (2008). The history of seasonally dry tropical forests in eastern South America: Inferences from the genetic structure of the tree *Astronium urundeuva* (Anacardiaceae). *Molecular Ecology*, 17(13), 3147-3159. <https://doi.org/10.1111/j.1365-294X.2008.03817.x>

Carstens, B. C., Brennan, R. S., Chua, V., Duffie, C. V., Harvey, M. G., Koch, R. A., & Sullivan, J. (2013). Model selection as a tool for phylogeographic inference: An example from the willow *Salix melanopsis*. *Molecular Ecology*, 22(15), 4014–4028. <https://doi.org/10.1111/mec.12347>

Catchen, J., Hohenlohe, P. A., Bassham, S., Amores, A., & Cresko, W. A. (2013). Stacks: An analysis tool set for population genomics. *Molecular Ecology*, 22(11), 3124–3140. <https://doi.org/10.1111/mec.12354>

Chapman, F. M. (1921). *The distribution of bird life in the Urubamba Valley of Peru. A Report on the Birds Collected by the Yale University-National Geographic Society's Expeditions*. Retrieved from <http://repository.si.edu//handle/10088/10044>

Claramunt, S., Derryberry, E. P., Remsen, J. V., & Brumfield, R. T. (2012). High dispersal ability inhibits speciation in a continental radiation of passerine birds. *Proceedings of the Royal Society B: Biological Sciences*, 279(1733), 1567–1574. <https://doi.org/10.1098/rspb.2011.1922>

Clark, P. U., Archer, D., Pollard, D., Blum, J. D., Rial, J. A., Brovkin, V., Mix, A. C., Pisias, N. G., & Roy, M. (2006). The middle Pleistocene transition: Characteristics, mechanisms, and implications for long-term changes in atmospheric pCO₂. *Quaternary Science Reviews*, 25(23), 3150–3184. <https://doi.org/10.1016/j.quascirev.2006.07.008>

Collevatti, R. G., Terribile, L. C., de Oliveira, G., Lima-Ribeiro, M. S., Nabout, J. C., Rangel, T. F., & Diniz-Filho, J. A. F. (2013). Drawbacks to palaeodistribution modelling: The case of South American seasonally dry forests. *Journal of Biogeography*, 40(2), 345–358. <https://doi.org/10.1111/jbi.12005>

Collevatti, R. G., Terribile, L. C., Lima-Ribeiro, M. S., Nabout, J. C., de Oliveira, G., Rangel, T. F., Rabelo, S. G., & Diniz-Filho, J. A. F. (2012). A coupled phylogeographical and species distribution modelling approach recovers the demographical history of a Neotropical seasonally dry forest tree species. *Molecular Ecology*, 21(23), 5845–5863. <https://doi.org/10.1111/mec.12071>

Cortes, A. L. A., Rapini, A., & Daniel, T. F. (2015). The Tetramerium lineage (Acanthaceae: Justicieae) does not support the Pleistocene Arc Hypothesis for South American seasonally dry forests. *American Journal of Botany*, 102(6), 992–1007. <https://doi.org/10.3732/ajb.1400558>

Danecek, P., Auton, A., Abecasis, G., Albers, C. A., Banks, E., DePristo, M. A., Handsaker, R. E., Lunter, G., Marth, G. T., Sherry, S. T., McVean, G., & Durbin, R. (2011). The variant call format and VCFtools. *Bioinformatics*, 27(15), 2156–2158. <https://doi.org/10.1093/bioinformatics/btr330>

Dawideit, B. A., Phillimore, A. B., Laube, I., Leisler, B., & Böhning-Gaese, K. (2009). Ecomorphological predictors of natal dispersal distances in birds. *Journal of Animal Ecology*, 78(2), 388–395. <https://doi.org/10.1111/j.1365-2656.2008.01504.x>

de Melo, W. A., Lima-Ribeiro, M. S., Terribile, L. C., & Collevatti, R. G. (2016). Coalescent simulation and paleodistribution modeling for *Tabebuia rosealba* do not support South American dry forest Refugia hypothesis. *PLoS One*, 11(7), e0159314. <https://doi.org/10.1371/journal.pone.0159314>

del Hoyo, J., Collar, N. J., Christie, D. A., Elliott, A., & Fishpool, L. D. C. (2017). *Illustrated Checklist of the Birds of the World: Passerines*. Lynx Edicions.

del Hoyo, J., Collar, N. J., Kirwan, G. M. (2017). Plain Thornbird (*Phacellodomus inornatus*). In J. del Hoyo, A. Elliott, J. Sargatal, D. A. Christie, & E. de Juana (Eds.), *Handbook of the Birds of the World Alive*. : Lynx Ediciones.

Derryberry, E. P., Claramunt, S., Derryberry, G., Chesser, R. T., Cracraft, J., Aleixo, A., Pérez-Emán, J., Remsen Jr., J. V., & Brumfield, R. T. (2011). Lineage diversification and morphological evolution in a large-scale continental radiation: The Neotropical ovenbirds and woodcreepers (Aves: Furnariidae). *Evolution*, 65(10), 2973–2986. <https://doi.org/10.1111/j.1558-5646.2011.01374.x>

Dickinson, E. C., & Christidis, L. (Eds.). (2014). *The Howard and Moore complete checklist of the birds of the world* (4th ed., Vol. 2). : Aves Press.

Drummond, A. J., & Rambaut, A. (2007). BEAST: Bayesian evolutionary analysis by sampling trees. *BMC Evolutionary Biology*, 7(1), 214. <https://doi.org/10.1186/1471-2148-7-214>

Earl, D. A., & vonHoldt, B. M. (2012). STRUCTURE HARVESTER: A website and program for visualizing STRUCTURE output and implementing the Evanno method. *Conservation Genetics Resources*, 4(2), 359–361. <https://doi.org/10.1007/s12686-011-9548-7>

Edgar, R. C. (2004). MUSCLE: Multiple sequence alignment with high accuracy and high throughput. *Nucleic Acids Research*, 32(5), 1792–1797. <https://doi.org/10.1093/nar/gkh340>

Edwards, S. V., Shultz, A. J., & Campbell-Staton, S. C. (2015). Next-generation sequencing and the expanding domain of phylogeography. *Folia Zoologica*, 64(3), 187–207. <https://doi.org/10.25225/fozo.v64.i3.a2.2015>

Evanno, G., Regnaut, S., & Goudet, J. (2005). Detecting the number of clusters of individuals using the software STRUCTURE: A simulation study. *Molecular Ecology*, 14(8), 2611–2620. <https://doi.org/10.1111/j.1365-294X.2005.02553.x>

Excoffier, L., & Lischer, H. E. L. (2010). Arlequin suite ver 3.5: A new series of programs to perform population genetics analyses under Linux and Windows. *Molecular Ecology Resources*, 10(3), 564–567. <https://doi.org/10.1111/j.1755-0998.2010.02847.x>

GBIF (2016). GBIF occurrence Download <https://doi.org/10.15468/dl.coho3g>

Haffer, J. (1967). Zoogeographical notes on the nonforest lowland bird faunas of Northwestern South America. *Hornero*, 10(4), 315–333.

Haffer, J. (1969). Speciation in Amazonian forest birds. *Science*, 165(3889), 131–137. <https://doi.org/10.1126/science.165.3889.131>

Harvey, M., Winger, B., Seeholzer, G., Cáceres, A. D. (2011). Avifauna of the Gran Pajonal and Southern Cerros Del Sira, Peru. *The Wilson Journal of Ornithology*, 123, 289–315. <https://doi.org/10.2307/23033397>

Hewitt, G. M. (1988). Hybrid zones-natural laboratories for evolutionary studies. *Trends in Ecology & Evolution*, 3(7), 158–167. [https://doi.org/10.1016/0169-5347\(88\)90033-X](https://doi.org/10.1016/0169-5347(88)90033-X)

Hickerson, M. J., Carstens, B. C., Cavender-Bares, J., Crandall, K. A., Graham, C. H., Johnson, J. B., Rissler, L., Victoriano, P. F., & Yoder, A. D. (2010). Phylogeography's past, present, and future: 10 years after Avise, 2000. *Molecular Phylogenetics and Evolution*, 54(1), 291–301. <https://doi.org/10.1016/j.ympev.2009.09.016>

Hijmans, R. J., Cameron, S. E., Parra, J. L., Jones, P. G., & Jarvis, A. (2005). Very high resolution interpolated climate surfaces for global land areas. *International Journal of Climatology*, 25(15), 1965–1978. <https://doi.org/10.1002/joc.1276>

Hilty, S. L. (2003). *Birds of Venezuela*, 2nd ed. Princeton University Press.

Hoorn, C., Wesselingh, F. P., ter Steege, H., Bermudez, M. A., Mora, A., Sevink, J., Sanmartin, I., Sanchez-Meseguer, A., Anderson, C. L., Figueiredo, J. P., Jaramillo, C., Riff, D., Negri, F. R., Hooghiemstra, H., Lundberg, J., Stadler, T., Sarkinen, T., & Antonelli, A. (2010). Amazonia through time: Andean uplift, climate change, landscape evolution, and biodiversity. *Science*, 330(6006), 927–931. <https://doi.org/10.1126/science.1194585>

Hughes, P. D., Gibbard, P. L., & Ehlers, J. (2013). Timing of glaciation during the last glacial cycle: Evaluating the concept of a global 'Last Glacial Maximum' (LGM). *Earth-Science Reviews*, 125, 171–198. <https://doi.org/10.1016/j.earscirev.2013.07.003>

Isler, M. L., Isler, P. R., & Brumfield, R. T. (2005). Clinal variation in vocalizations of an antbird (Thamnophilidae) and implications for defining species limits. *The Auk*, 122(2), 433–444. <https://doi.org/10.1093/auk/122.2.433>

Isler, M. L., Isler, P. R., & Whitney, B. M. (1998). Use of vocalizations to establish species limits in antbirds (Passeriformes: Thamnophilidae). *The Auk*, 115(3), 577–590. <https://doi.org/10.2307/4089407>

Jakobsson, M., & Rosenberg, N. A. (2007). CLUMPP: A cluster matching and permutation program for dealing with label switching and multimodality in analysis of population structure. *Bioinformatics*, 23(14), 1801–1806. <https://doi.org/10.1093/bioinformatics/btm233>

Jombart, T. (2008). adegenet: A R package for the multivariate analysis of genetic markers. *Bioinformatics*, 24(11), 1403–1405. <https://doi.org/10.1093/bioinformatics/btn129>

Kamm, J., Terhorst, J., Durbin, R., & Song, Y. S. (2019). Efficiently inferring the demographic history of many populations with allele count data. *Journal of the American Statistical Association*, 115(531), 1472–1487. <https://doi.org/10.1080/01621459.2019.1635482>

Keasey, M., Moir, R., Wilson, A., Stones-Havas, S., Cheung, M., Sturrock, S., Buxton, S., Cooper, A., Markowitz, S., Duran, C., Thierer, T., Ashton, B., Meintjes, P., & Drummond, A. (2012). Geneious Basic: An integrated and extendable desktop software platform for the organization and analysis of sequence data. *Bioinformatics*, 28(12), 1647–1649. <https://doi.org/10.1093/bioinformatics/bts199>

Kipp, F. A. (1959). Der handflügel-index als flugbiologisches Maß. *Vogelwarte*, 20, 77–86.

Klicka, J., & Zink, R. M. (1997). The importance of recent ice ages in speciation: A failed paradigm. *Science*, 277(5332), 1666–1669. <https://doi.org/10.1126/science.277.5332.1666>

Lanna, F. M., Werneck, F. P., Gehara, M., Fonseca, E. M., Colli, G. R., Sites, J. W., Rodrigues, M. T., & Garda, A. A. (2018). The evolutionary history of Lygodactylus lizards in the South American open diagonal. *Molecular Phylogenetics and Evolution*, 127, 638–645. <https://doi.org/10.1016/j.ympev.2018.06.010>

Lawson, D. J., van Dorp, L., & Falush, D. (2018). A tutorial on how not to over-interpret STRUCTURE and ADMIXTURE bar plots. *Nature Communications*, 9(1), 3258. <https://doi.org/10.1038/s41467-018-05257-7>

Leigh, J. W., & Bryant, D. (2015). popart: Full-feature software for haplotype network construction. *Methods in Ecology and Evolution*, 6(9), 1110–1116. <https://doi.org/10.1111/2041-210X.12410>

Linares-Palomino, R. (2006). Phyogeography and floristics of seasonally dry tropical forests in Peru. In R. T. Pennington & J. A. Ratter (Eds.), *Neotropical Savannas and Seasonally Dry Forests: Plant Diversity, Biogeography, and Conservation*, (pp. 257–279). Boca Raton, FL: CRC Press.

Linck, E., & Battey, C. J. (2019). Minor allele frequency thresholds strongly affect population structure inference with genomic data sets. *Molecular Ecology Resources*, 19(3), 639–647. <https://doi.org/10.1111/1755-0998.12995>

Lisiecki, L. E., & Raymo, M. E. (2005). A Pliocene-Pleistocene stack of 57 globally distributed benthic $\delta^{18}\text{O}$ records. *Paleoceanography*, 20(1). <https://doi.org/10.1029/2004PA001071>

Mayle, F. E. (2004). Assessment of the Neotropical dry forest refugia hypothesis in the light of palaeoecological data and vegetation model simulations. *Journal of Quaternary Science*, 19(7), 713–720. <https://doi.org/10.1002/jqs.887>

McCormack, J. E., Hird, S. M., Zellmer, A. J., Carstens, B. C., & Brumfield, R. T. (2013). Applications of next-generation sequencing to phylogeography and phylogenetics. *Molecular Phylogenetics and Evolution*, 66(2), 526–538. <https://doi.org/10.1016/j.ympev.2011.12.007>

Mogni, V. Y., Oakley, L. J., & Prado, D. E. (2015). The distribution of woody legumes in Neotropical dry forests: The Pleistocene Arc theory 20 years on. *Edinburgh Journal of Botany*, 72(1), 35–60. <https://doi.org/10.1017/S0960428614000298>

Moraes, E. M., Yotoko, K. S. C., Manfrin, M. H., Solferini, V. N., & Sene, F. M. (2009). Phylogeography of the cactophilic species *Drosophila gouveai*: Demographic events and divergence timing in dry vegetation enclaves in Eastern Brazil. *Journal of Biogeography*, 36(11), 2136–2147. <https://doi.org/10.1111/j.1365-2699.2009.02145.x>

Naka, L. N., & Brumfield, R. T. (2018). The dual role of Amazonian rivers in the generation and maintenance of avian diversity. *Science Advances*, 4(8), eaar8575. <https://doi.org/10.1126/sciadv.aar8575>

Nater, A., Greminger, M. P., Arora, N., van Schaik, C. P., Goossens, B., Singleton, I., Verschoor, E. J., Warren, K. S., & Krützen, M. (2015). Reconstructing the demographic history of orang-utans using approximate Bayesian computation. *Molecular Ecology*, 24(2), 310–327. <https://doi.org/10.1111/mec.13027>

Oswald, J. A., Overcast, I., Mauck, W. M., Andersen, M. J., & Smith, B. T. (2017). Isolation with asymmetric gene flow during the nonsynchronous divergence of dry forest birds. *Molecular Ecology*, 26(5), 1386–1400. <https://doi.org/10.1111/mec.14013>

Oswald, J. A., & Steadman, D. W. (2015). The changing diversity and distribution of dry forest passerine birds in northwestern Peru since the last ice age. *The Auk*, 132(4), 836–862. <https://doi.org/10.1642/AUK-15-74.1>

Pelletier, T. A., & Carstens, B. C. (2014). Model choice for phylogeographic inference using a large set of models. *Molecular Ecology*, 23(12), 3028–3043. <https://doi.org/10.1111/mec.12722>

Pennington, R. T., Lavin, M., Prado, D. E., Pendry, C. A., Pell, S. K., & Butterworth, C. A. (2004). Historical climate change and speciation: Neotropical seasonally dry forest plants show patterns of both tertiary and quaternary diversification. *Philosophical Transactions of the Royal Society of London. Series B, Biological Sciences*, 359(1443), 515–537. <https://doi.org/10.1098/rstb.2003.1435>

Pennington, R. T., Lewis, G. P., & Ratter, J. A. (2006). An overview of the plant diversity, biogeography and conservation of Neotropical savannas and seasonally dry forests. In R. T. Pennington & J. A. Ratter (Eds.), *Neotropical Savannas and Dry Forests: Plant diversity, biogeography, and conservation* (pp. 1–29). Boca Raton, FL: CRC Press.

Pennington, R. T., Prado, D. E., & Pendry, C. A. (2000). Neotropical seasonally dry forests and Quaternary vegetation changes. *Journal of Biogeography*, 27(2), 261–273. <https://doi.org/10.1046/j.1365-2699.2000.00397.x>

Peterson, B. K., Weber, J. N., Kay, E. H., Fisher, H. S., & Hoekstra, H. E. (2012). Double digest RADseq: An inexpensive method for de novo SNP discovery and genotyping in model and non-model species. *PLoS One*, 7(5), e37135. <https://doi.org/10.1371/journal.pone.0037135>

Petit, J. R., Jouzel, J., Raynaud, D., Barkov, N. I., Barnola, J.-M., Basile, I., Bender, M., Chappellaz, J., Davis, M., Delaygue, G., Delmotte, M., Kotlyakov, V. M., Legrand, M., Lipenkov, V. Y., Lorius, C., PÉpin, L., Ritz, C., Saltzman, E., & Stievenard, M. (1999). Climate and atmospheric history of the past 420,000 years from the Vostok ice core, Antarctica. *Nature*, 399(6735), 429–436. <https://doi.org/10.1038/20859>

Phillips, S. J., Anderson, R. P., & Schapire, R. E. (2006). Maximum entropy modeling of species geographic distributions. *Ecological Modelling*, 190(3), 231–259. <https://doi.org/10.1016/j.ecolmodel.2005.03.026>

Prado, D. E. (1991). *A critical evaluation of the floristic links between Chaco and Caatingas vegetation in South America* (Thesis, University of St Andrews). University of St Andrews. Retrieved from <https://research-repository.st-andrews.ac.uk/handle/10023/14121>

Prado, D. E., & Gibbs, P. (1993). Patterns of species distributions in the dry seasonal forests of South America. *Annals of the Missouri Botanical Garden*, 80, 902–927. <https://doi.org/10.2307/2399937>

Price, T. (2008). *Speciation in birds*, Greenwood Village, Co: Roberts & Co.

Pritchard, J. K., Stephens, M., & Donnelly, P. (2000). Inference of population structure using multilocus genotype data. *Genetics*, 155(2), 945–959.

QGIS Development Team (2017). QGIS geographic information system. Open Source Geospatial Foundation Project.

Quijada-Mascareñas, J. A., Ferguson, J. E., Pook, C. E., Salomão, M. D. G., Thorpe, R. S., & Wüster, W. (2007). Phylogeographic patterns of trans-Amazonian vicariants and Amazonian biogeography: The Neotropical rattlesnake (*Crotalus durissus* complex) as an

example. *Journal of Biogeography*, 34(8), 1296–1312. <https://doi.org/10.1111/j.1365-2699.2007.01707.x>

Rambaut, A., Drummond, A. J., Xie, D., Baele, G., & Suchard, M. A. (2018). Posterior summarization in Bayesian phylogenetics using tracer 1.7. *Systematic Biology*, 67(5), 901–904. <https://doi.org/10.1093/sysbio/syy032>

Remsen, J. V. (2003a). Family Furnariidae (Ovenbirds). In J. del Hoyo, A. Elliott, & D. A. Christie (Eds.), *Handbook of the Birds of the World: Volume 8: Broadbills to Tapaculos*. Lynx Edicions.

Remsen, J. V. (2003b). *Proposal 41 to South American checklist committee: Split Phacellodomus inornatus from P. rufifrons*. Retrieved from <http://www.museum.lsu.edu/~Remsen/SACCprop41.htm>

Remsen, J. V. (2005). Pattern, process, and rigor meet classification. *The Auk*, 122(2), 403–413. <https://doi.org/10.1093/auk/122.2.403>

Richards, C. L., Carstens, B. C., & Knowles, L. L. (2007). Distribution modelling and statistical phylogeography: An integrative framework for generating and testing alternative biogeographical hypotheses. *Journal of Biogeography*, 34(11), 1833–1845. <https://doi.org/10.1111/j.1365-2699.2007.01814.x>

Ridgely, R. S., & Tudor, G. (2009). *Field guide to the Songbirds of South America: The Passerines* (1st ed.). University of Texas Press.

Rosenberg, N. A. (2004). *distruct: A program for the graphical display of population structure*. *Molecular Ecology Notes*, 4(1), 137–138. <https://doi.org/10.1046/j.1471-8286.2003.00566.x>

Rull, V. (2011). Neotropical biodiversity: Timing and potential drivers. *Trends in Ecology & Evolution*, 26(10), 508–513. <https://doi.org/10.1016/j.tree.2011.05.011>

Särkinen, T., Iganci, J. R., Linares-Palomino, R., Simon, M. F., & Prado, D. E. (2011). Forgotten forests - issues and prospects in biome mapping using seasonally dry tropical forests as a case study. *BMC Ecology*, 11(1), 27. <https://doi.org/10.1186/1472-6785-11-27>

Savit, A. Z., & Bates, J. M. (2015). Right around the Amazon: The origin of the circum-Amazonian distribution in *Tangara cayana*. *Folia Zoologica*, 64(3), 273–283. <https://doi.org/10.2522/fozo.v64.i3.a8.2015>

Seddon, N., & Tobias, J. A. (2007). Song divergence at the edge of Amazonia: An empirical test of the peripatric speciation model. *Biological Journal of the Linnean Society*, 90(1), 173–188. <https://doi.org/10.1111/j.1095-8312.2007.00753.x>

Shackleton, N. J., & Opdyke, N. D. (1976). Oxygen-Isotope and Paleomagnetic Stratigraphy of Pacific Core V28-239, Late Pliocene to Latest Pleistocene. In *Geological Society of America Memoirs: Vol. 145. Investigation of Late Quaternary Paleoceanography and Paleoclimatology*.

Sheard, C., Neate-Clegg, M. H. C., Alioravainen, N., Jones, S. E. I., Vincent, C., MacGregor, H. E. A., Bregman, T. P., Claramunt, S., & Tobias, J. A. (2020). Ecological drivers of global gradients in avian dispersal inferred from wing morphology. *Nature Communications*, 11(1), 2463. <https://doi.org/10.1038/s41467-020-16313-6>

Silva, J. M. C. D., & Bates, J. M. (2002). Biogeographic patterns and conservation in the South American Cerrado: A tropical savanna hotspot. *BioScience*, 52(3), 225–234. [https://doi.org/10.1641/0006-3568\(2002\)052\[0225:BPACIT\]2.0.CO;2](https://doi.org/10.1641/0006-3568(2002)052[0225:BPACIT]2.0.CO;2)

Skutch, A. F. (1969). A study of the Rufous-fronted Thornbird and associated birds: Part 1. Life history of the Rufous-fronted Thornbird. *The Wilson Bulletin*, 81(1), 5–43.

Smith, B. T., McCormack, J. E., Cuervo, A. M., Hickerson, M. J., Aleixo, A., Cadena, C. D., & Brumfield, R. T. (2014). The drivers of tropical speciation. *Nature*, 515(7527), 406–409. <https://doi.org/10.1038/nature13687>

Termignoni-García, F., Jaramillo-Correa, J. P., Chablé-Santos, J., Liu, M., Shultz, A. J., Edwards, S. V., & Escalante-Pliego, P. (2017). Genomic footprints of adaptation in a cooperatively breeding tropical bird across a vegetation gradient. *Molecular Ecology*, 26(17), 4483–4496. <https://doi.org/10.1111/mec.14224>

Tobias, J., Brawn, J., Brumfield, R., Derryberry, E., Kirschel, A., & Seddon, N. (2012). The importance of suboscine birds as study systems in ecology and evolution. *Ornithologia Neotropical*, 23, 161–174.

Vásquez, F., Grandez Casado, J., Muñoz-Pizango, E. G., García-Villacorta, R., & Gagliardi-Urrutia, G. (2018). Bird diversity in the seasonally dry forests of central Huallaga, Peru. *Cotinga*, 40, 31–43.

Warren, D. L., Glor, R. E., & Turelli, M. (2010). ENMTools: A toolbox for comparative studies of environmental niche models. *Ecography*, 33(3), 607–611. <https://doi.org/10.1111/j.1600-0587.2009.06142.x>

Watanabe, S., Hajima, T., Sudo, K., Nagashima, T., Takemura, T., Okajima, H., Nozawa, T., Kawase, H., Abe, M., Yokohata, T., Ise, T., Sato, H., Kato, E., Takata, K., Emori, S., & Kawamiya, M. (2011). MIROC-ESM 2010: Model description and basic results of CMIP5-20c3m experiments. *Geoscientific Model Development*, 4(4), 845–872. <https://doi.org/10.5194/gmd-4-845-2011>

Weir, J. T., & Schlüter, D. (2007). The latitudinal gradient in recent speciation and extinction rates of birds and mammals. *Science*, 315(5818), 1574–1576. <https://doi.org/10.1126/science.1135590>

Weir, J. T., & Schlüter, D. (2008). Calibrating the avian molecular clock. *Molecular Ecology*, 17(10), 2321–2328. <https://doi.org/10.1111/j.1365-294X.2008.03742.x>

Werneck, F. P., Costa, G. C., Colli, G. R., Prado, D. E., & Sites, J. W. (2011). Revisiting the historical distribution of seasonally dry tropical forests: new insights based on palaeodistribution modelling and palynological evidence. *Global Ecology and Biogeography*, 20(2), 272–288.

Werneck, F. P., Gamble, T., Colli, G. R., Rodrigues, M. T., & Sites, J. W. (2012). Deep diversification and long-term persistence in the South American “Dry Diagonal”: Integrating continent-wide phylogeography and distribution modeling of geckos. *Evolution*, 66(10), 3014–3034.

Werneck, F. P., Giugliano, L. G., Collevatti, R. G., & Colli, G. R. (2009). Phylogeny, biogeography and evolution of clutch size in South American lizards of the genus *Kentropyx* (Squamata: Teiidae). *Molecular Ecology*, 18(2), 262–278. <https://doi.org/10.1111/j.1365-294X.2008.03999.x>

Willis, K. J., & Whittaker, R. J. (2000). The refugial debate. *Science*, 287(5457), 1406–1407. <https://doi.org/10.1126/science.287.5457.1406>

Winger, B. M., Hosner, P. A., Bravo, G. A., Cuervo, A. M., Aristizábal, N., Cueto, L. E., & Bates, J. M. (2015). Inferring speciation history in the Andes with reduced-representation sequence data: An example in the bay-backed antpittas (Aves; Grallariidae; *Grallaria hypoleuca* s. l.). *Molecular Ecology*, 24(24), 6256–6277. <https://doi.org/10.1111/mec.13477>

SUPPORTING INFORMATION

Additional supporting information may be found online in the Supporting Information section.

How to cite this article: Corbett EC, Bravo GA, Schunck F, Naka LN, Silveira LF, Edwards SV. Evidence for the Pleistocene Arc Hypothesis from genome-wide SNPs in a Neotropical dry forest specialist, the Rufous-fronted Thornbird (Furnariidae: *Phacellodomus rufifrons*). *Mol Ecol* 2020;29:4457–4472. <https://doi.org/10.1111/mec.15640>